Monitoring of a Full-Scale Wing Fatigue Test

Jaap Heida, Jason Hwang

MONITORING OF A FULL-SCALE WING FATIGUE TEST

Jaap Heida, Jason Hwang

National Aerospace Laboratory NLR, Voorsterweg 31, 8316 PR Marknesse, The Netherlands

jaap.heida@nlr.nl

ABSTRACT

A wing of a decommissioned aircraft of the Royal Netherlands Air Force (RNLAF) was fatigue tested to more than two times the design life. Part of the test was the evaluation of load monitoring and Structural Health Monitoring (SHM) techniques. For load monitoring the data of conventional resistance strain gauges was compared with the response of optical Fibre Bragg Gratings (FBG). For SHM the Acoustic Emission (AE) and Comparative Vacuum Monitoring (CVM) techniques were employed to monitor fatigue crack initiation and growth. With the optical fibres a linear correlation between the FBG's and the conventional strain gauges was obtained using a specific strain transfer factor. The SHM techniques, on the other hand, were less successful. For the CVM technique no cracks occurred at the locations under periodic monitoring (but also no false calls occurred during the complete test). Further, the AE system under continuous monitoring registered a lot of AE activity from different sources (also after drastic filtering of the AE data) but the AE data could not be reliably related to the initiation and growth of fatigue cracks in the areas monitored. Most of the AE activity was probably caused by mechanically induced noise such as frictional noise from the fastener locations and other surface rubbing areas.

KEYWORDS : *load monitoring, structural health monitoring, optic fibre Bragg grating, acoustic emission, comparative vacuum monitoring*

INTRODUCTION

The left-hand side wing of a decommissioned F-16 Block 15 aircraft of the RNLAF was fatigue tested to more than two times the design life. The main objective of the test was to determine whether the ex-service wing contained damage not accounted for in the early durability test programme that was performed in the late 1970s or in the current durability and damage tolerance analysis of Lockheed Martin (LM). Other objectives were to generate data (e.g. crack growth curves for critical locations) that can be used for an assessment of the current inspection programme and to establish the most likely failure scenario, including an estimate of the associated technical end of life time [1].

Part of the fatigue test was the evaluation of load monitoring and structural health monitoring (SHM) techniques. For load monitoring during the fatigue test the data of conventional resistance strain gauges (single gauges, full bridges) was compared with the response of optical FBG sensors. A total of 19 FBG's were installed on the upper wing skin, divided over three fibres. SHM techniques are employed in-service to assess the real-time condition of a structure. For SHM the AE and CVM techniques were employed during the fatigue test to monitor fatigue crack initiation and growth. AE continuous monitoring was done with a 16-channel AE system and resonant sensors (150 kHz) covering five critical locations on the upper and lower wing skin. A CVM laboratory system was used for fatigue crack detection at the lower wing attachment fittings under periodic monitoring. Figure 1 gives a schematic overview of the upper wing skin with the location of the FBG and AE sensors (CVM sensors on the lower skin).

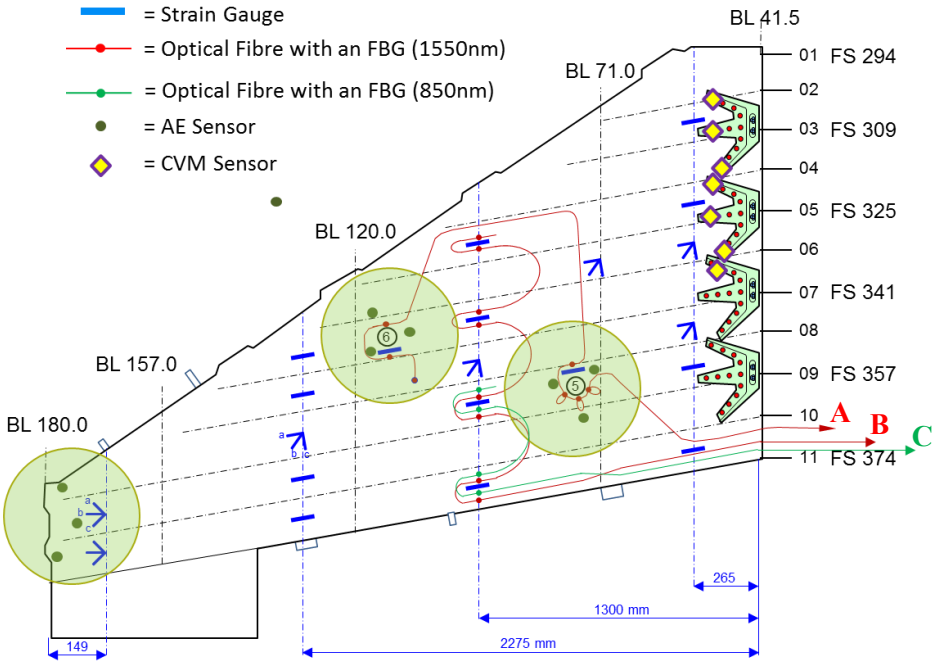

Figure 1: Monitoring of the upper wing skin with AE and FBG sensors (CVM on the lower skin)

1 TEST ARTICLE AND WING TEST SETUP

The test article for the fatigue test was the left-hand wing of a decommissioned F-16 Block 15 aircraft of the RNLAF that had accumulated 4200 flight hours (Fig. 2). The aircraft had been subjected to different modification programs implying e.g. the installation of new Al-Li wing attachment fittings (WAF). The test article only comprised the wing box, the fixed trailing edge and the eight WAF's with the total of 16 bolts that connect the wing to the fuselage. Not included were the flaperon, the leading edge flap (LEF) and the rotary actuators that connect the LEF to the wing box. No artificial damages were applied to the test article. Only naturally existing damages, caused by in-service fatigue loading, corrosion, tool marks, etc. were considered.

Figure 2: Impression of the F-16 Block 15 wing test setup

The static and fatigue loads on the wing box were introduced by a total of 23 force-controlled hydraulic actuators. An overview of the wing test setup is given in Figure 2 illustrating the complex layout of the different actuators. The wing root was mounted to a steel test frame in such a way that the wing interface loads over the WAF's were similar to that in the real aircraft. The validity of the representative wing root support was dealt with using calculations with the F-16 Block 15 coarse grid Finite Element Model (cgFEM) of LM that was available at the NLR

The fatigue test was carried out under room temperature ambient conditions. The aim of the test was to cover two lifetimes (16,000 flight hours) or less in case of untimely failure. The load spectrum was based on a spectrum as used by LM in the development of the current Fleet Structural Maintenance Plan (FSMP) for the RNLAF. The spectrum consisted of consecutive blocks of 500 simulated flight hours (or 412 flights). Marker loads (ML) were added to the spectrum to improve the readability of the fatigue crack surfaces for post-test quantitative fractography. Prior to the start of the test, a set of commissioning load cases were applied to verify the correct functioning of the test setup. In addition, during the test strain surveys were performed at discrete moments in time (roughly each 2000 flight hours). The strain surveys were meant to generate strain data for the correlation of the F-16 Block 15 cgFEM that will be used for further processing of the durability test results, and to monitor the possible changing of load paths due to the growth of fatigue cracks [1].

Prior to the start of the test also an extensive non-destructive inspection (NDI) of all relevant structural areas was performed. The result of this inspection was that no anomalies such as cracks were detected for all wing areas designated for the FBG monitoring and SHM measurements.

2 FBG LOAD MONITORING

The main goal of this study was to evaluate the performance of the optical fibres as a load monitoring technology over a long-term fatigue loading environment. In order to achieve this goal, coupon tests have been executed prior to the fatigue testing [2]. The coupon tests aimed to develop procedures to apply optical fibres on a complex structure such as the F-16 wing. For example, the correct combination of the adhesive and the cladding of the fibre were assessed (polyamide cladding with M-Bond 200 or a 2-component X60 adhesive). Based on the results of the coupon tests, three optical fibres with in total 19 FBG's were attached to the F-16 upper wing surface, see Figures 1 and 3 [3]. Table 1 gives more details on the optical fibres used.

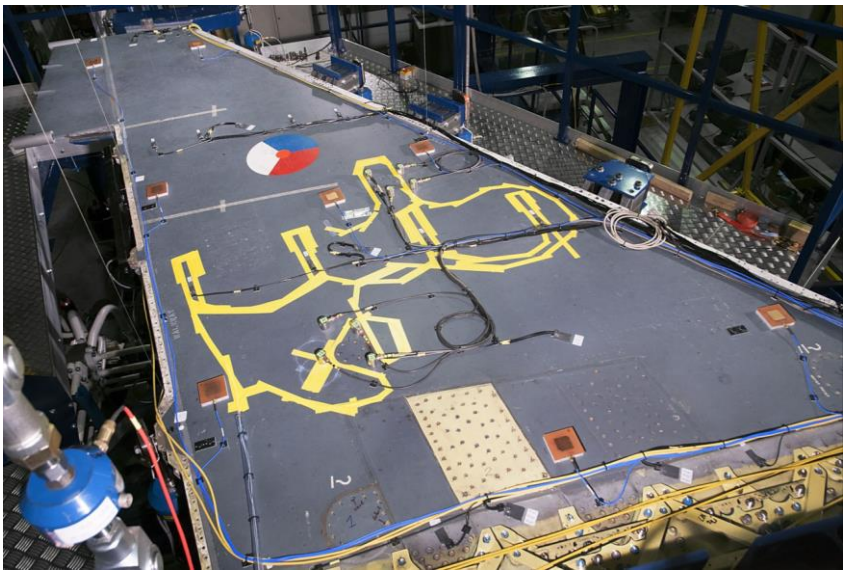

Figure 3: Load monitoring with optical FBG's on the upper skin (fibres under yellow tape for protection)

Table 1. List of optical fibres used during the F-16 Fatigue Test Campaign

Fibre	Spectral range	# FBGs	Purpose	Interrogator
A	1529–1576 nm	7	Wing-skin cut-out monitoring, temperature measurement	IFIS100
B	1522–1578 nm	8	Comparison with strain gauges	IFIS100
C	839–860 nm	4	Comparison with strain gauges	Deminsys Ultra

Two distinctive FBG interrogator systems were used in the test, an IFIS100 system of the Korean company Fiberpro, Inc. and a Deminsys Ultra system of the Dutch company Technobis Fibre Technologies, see Table 2.

Table 2. Summary of the two FBG interrogator systems used

Interrogators:	Fiberpro IFIS100	Technobis Deminsys Ultra
Wavelength range / accuracy	1510–1595 nm / 20 pm	830–870 nm / 4–17 pm
Wavelength resolution / repeatability	1 pm / < 3 pm	1.7 pm / < 2 pm

FBG measurements were performed during the execution of the static load sequences in the fatigue test (roughly each 2000 flight hours). Prior to the test campaign the strain transfer factor (SFT) of all FBG's was determined in a separate static test by correlating the strain measurements from conventional strain gauges and the FBG's. This has led to a certain "footprint" of all FBG's. The STF is a constant factor compensating for the strain transfer loss between the test specimen and the glass core [4]. It was noted that the STF of all FBG's in the same optical fibre were close to each other. However, between the optical fibres, large deviations in STF were observed (from 1.00 to 1.37). Nevertheless, the strain measurements during the fatigue test were performed until 16,000 flight hours (FH) using this STF footprint.

FBG readings were made during the stepwise increase and subsequent decrease of the static loading. Rabelo Faria [2] and Hwang [5] present the results and conclusions from this test campaign in more detail. Table 3 summarizes the maximal measurement error for five FBG's during a static load case. Fibre C was not taken into account due to fibre breakage (handling error). The average absolute error percentage was 1.28% and 97% of all FBG strain measurements were within ±5% of the strain gauge measurements. The results show that FBG's can withstand many cyclic load conditions when polyamide cladding is used. Furthermore, X60 covered FBG's showed no big differences compared to other M-Bond 200 bonded FBG's. In practice, X60 might be preferable since the optical fibre is then physically not exposed to the environment.

Table 3. Maximal error measured during the static load cases after certain flight hours flown (FH)

FBG #	Remark	STF	5k FH	8k FH	16k FH
A4	Hole # 5	1.31	1.76%	2.39%	3.69%
A6	Hole #6	1.31	1.71%	0.84%	2.82%
B2	Only M-200	1.01	3.48%	2.35%	1.66%
B4	M-200, X-60 covered	1.01	6.29%	4.62%	6.24%
B7	Only M-200	1.01	4.66%	8.86%	4.20%

The large STF discrepancy between the fibres A and B is remarkable. It was confirmed from the optical fibre supplier that the fibres A and B were from different manufacturer. Unfortunately, it was not possible to explain the discrepancy due to lack of information from the supplier.

3 STRUCTURAL HEALTH MONITORING

3.1 Comparative vacuum monitoring

A CVM™ laboratory system of Structural Monitoring Systems was used for fatigue crack detection at the lower wing attachment fittings. The system consists of a reference vacuum source (Kvac-5), a sensitive flow meter (SIM-8), a laptop for data logging and the self-adhesive CVM sensor with vacuum channel, see Figure 4. The flow meter measures any reduction of the vacuum level in the sensor channel, for example when a crack develops in the sensor area.

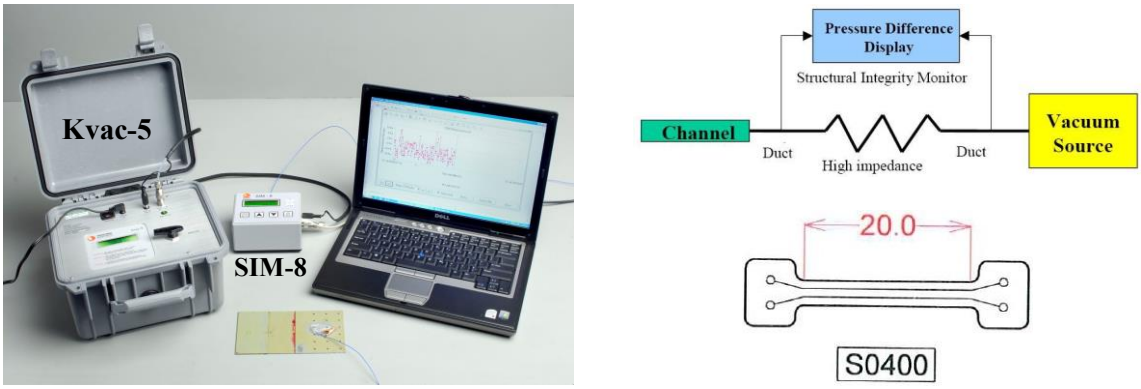

Figure 4: CVM laboratory system with S0400 intercept sensor

In total nine S0400 intercept CVM sensors were used to periodically monitor the 'finger' areas of the WAF's on the lower wing skin, see Figure 5. During the complete fatigue test no crack indications were obtained by the CVM system. But, inspection during and after the test showed that although cracks occurred in the fittings and in the bolt holes connecting the fittings to the wing skin, no cracks had in fact occurred at the locations under CVM monitoring. A positive result of the CVM measurements was that no false calls occurred during the complete test.

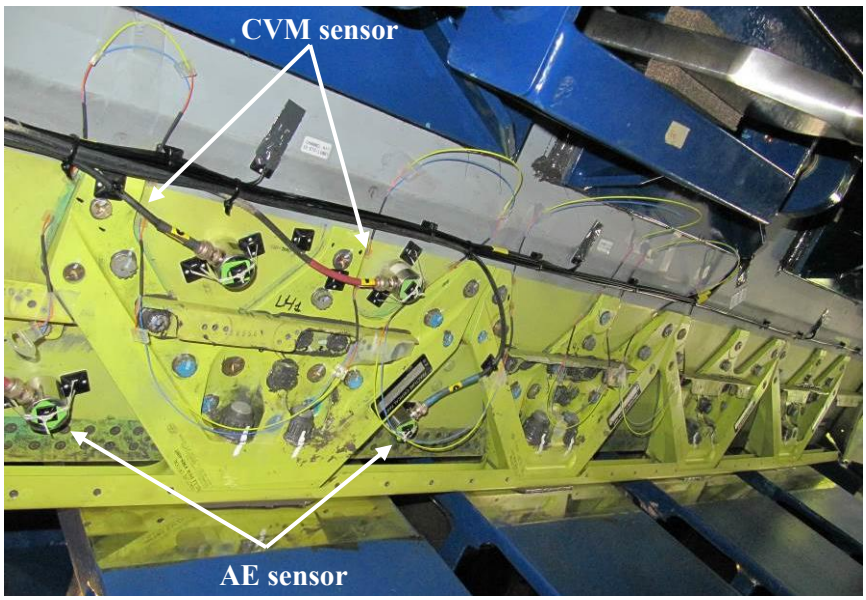

Figure 5: CVM monitoring of the 'finger' areas of the WAF's on the lower wing skin

3.2 Acoustic emission

AE monitoring was done with a 16-channel SAMOS 24 system (Physical Acoustics Corporation) and 16 resonant sensors (150 kHz) covering five critical locations on the upper and lower wing skin. Three locations were on the upper wing skin (two cut-out areas and the wing tip rib, Figs. 1 and 3) and two locations on the lower wing skin (LEF #2 and the forward WAF, Fig. 5). The sensors were attached to the surface with an electric hot glue gun using a hot melt adhesive. After some initial bonding problems, all sensors functioned well during the complete fatigue test. Calibration of the sensors was performed by checking the consistency of AE activity from lead-pencil breaks at different locations. Standard AE signal characteristics and two parameters were recorded, viz. the parameter load (for measurements during the strain surveys) and the number of fatigue test blocks.

The AE sensors were divided over the five locations of interest. For the WAF location four sensors were used and for the other locations three sensors each. The sensors were positioned in such a way to determine the source location of AE events using the 2D planar location mode of the SAMOS AE system. A minimum of three AE hits (from different sensors) was selected in the Location Setup module to determine the location of the AE event (3 Hits/Event). Proper functioning of the event location module was again done by lead-pencil breaks at different locations. However, for each AE group specific values for the effective wave velocity (ranging from 3000 to 4000 m/s) and other location parameters had to be determined.

AE measurements during the test were done continuously but, for practical and safety reasons, the recording was done in subsequent software files with duration of 24 hours. During the test a lot of AE activity combined with high amplitudes of the hits (up to 100 dB) was observed for all five AE groups. Figure 6 (left) gives an example for the AE event registration for sensor group 5, one of the cut-out areas on the upper wing skin (Fig. 1) in a test phase when there were no fatigue cracks in the structure yet. There is a lot of AE activity (155,917 events) and there are straight lines of AE events visible that are most certainly spurious event indications.

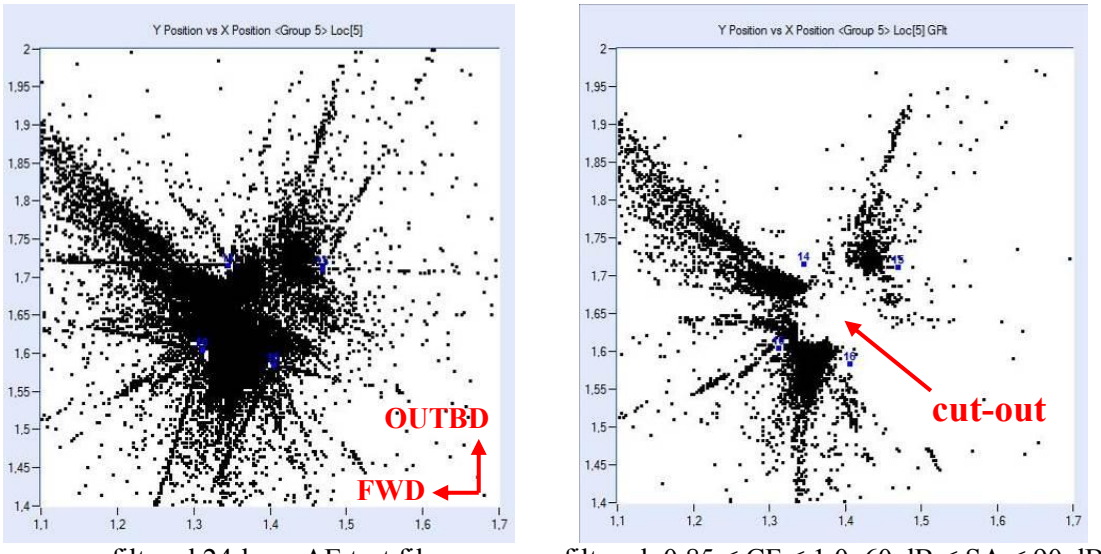

unfiltered 24-hour AE test file — filtered: 0.85 ≤ CF ≤ 1.0, 60 dB ≤ SA ≤ 90 dB

Figure 6: AE event location plots for a cut-out area on the upper wing skin. No cracks in the structure yet

The high AE activity is probably caused by external noise (e.g. from the hydraulic loading actuators) and internal noise coming from e.g. surface rubbing at the fastener locations. Anyway, audible noise was clearly present during the test. A solution could be the use of higher-frequency AE sensors and/or the application of AE hardware front-end filters (e.g. a high-pass filter). This would remove for example frequencies below 100 kHz which includes most audible noise [6, 7].

Higher-frequency AE-sensors, however, were not available for the present test. It was therefore decided to continue monitoring with the 150 kHz resonant sensors but to improve the event location performance by reducing the number of AE groups to four groups with four sensors each and to impose more stringent graphical filter settings.

The three sensors at the wing tip rib were removed and divided over the other three groups with three sensors. Calibration of AE signals was repeated after the rearrangement of the sensor groups. Now, a more stringent Location Setup setting was used for the AE event source location plots. Instead of a minimum of three now a minimum of four AE hits (from the four different sensors) was selected to determine the location of the AE event (4 Hits/Event). Furthermore, the following graphical filters were used for the event location plots:

- Correlation Factor (CF) that checks the correspondence between the location results of the four different subsets of three sensors. Trials were done with different minimum values for CF and finally a high value of 0.85 was selected ($0.85 \leq CF \leq 1.0$).
- Source Amplitude (SA) that checks for each localised event whether the hit amplitude at the source for all sensors satisfies a certain condition. For the present measurements it was assumed that a fatigue crack produces hits with amplitude larger than 60 dB and smaller than 90 dB, hence the requirement $60\ dB \leq SA \leq 90\ dB$.

The influence of the changes in the AE source Location Setup module and the implementation of graphical filters is illustrated in Figure 6 (right) for the same 24-hour test file of the cut-out area on the upper wing skin. The difference between the two plots is striking and the straight lines of spurious event indications have disappeared. Furthermore, the contour of the cut-out between the four sensors is now clearly visible. However, the number of events in the location plots is still considerable (28,538 events) and the question remained whether the location plots yield relevant information about fatigue crack initiation and growth. Therefore, the AE data were further analysed for cases with confirmed crack history.

For both cut-out areas on the upper wing skin fatigue cracks developed during the fatigue test. However, the AE event location plots for 24-hour data files in a test phase when fatigue cracks definitively had initiated in the structure (crack length larger than 2 mm) did not differ significantly from the plots with no cracks present, for example Figure 6 (right). On the other hand, for the WAF area on the lower wing skin differences were observed, see Figure 7. The differences in the AE event location plots at different test phases, however, could not be reliably related to the location and initiation time of the fatigue cracks detected with NDI.

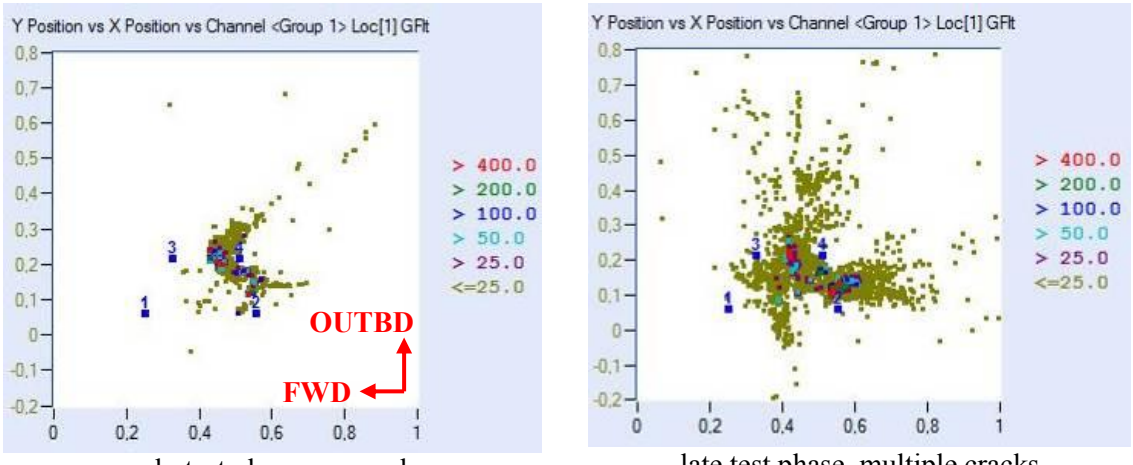

early test phase, no cracks | late test phase, multiple cracks

Figure 7: AE event location plots for the WAF area on the lower wing skin (AE sensors 1-4)

Finally, all AE 24-hour data files were linked to one total test file. For that purpose, data file filters were employed on the original files to decrease the size of the total data file (max 2 GB allowed). Different filters were evaluated, for example on the energy and average frequency, and the resulting files further analysed. Some trends in the AE activity versus time or number of fatigue test blocks could be observed but they could not be reliably related to the fatigue cracking detected with NDI.

CONCLUSIONS

The following conclusions were drawn from the monitoring of the full-scale wing fatigue test:

- With the optical fibres a linear correlation between the FBG's and the conventional strain gauges was obtained using a specific strain transfer factor.
- For the CVM technique no cracks occurred at the locations under periodic monitoring. But, also no false calls occurred during the complete test.
- The AE system under continuous monitoring registered a lot of AE activity from different sources (also after drastic filtering of the AE data) but the AE data could not be reliably related to the initiation and growth of fatigue cracks in the areas monitored. Most of the AE activity was probably non-relevant and caused by mechanically induced noise such as frictional noise from the fastener locations and other surface rubbing areas.

ACKNOWLEDGEMENTS

The authors would like to acknowledge the support and funding of the Defence Materiel Organisation (DMO) of the Ministry of Defence (MoD) in The Netherlands. Furthermore, the Agency for Defense Development of the Republic of Korea is also gratefully acknowledged for their support on various SHM activities.

REFERENCES

[1] M.J. Bos, J.S. Hwang, F.P. Grooteman, J.A.J.A. Dominicus, C.Y. Park. Load monitoring and structural health monitoring within the Royal Netherlands Air Force, *22nd Int. Aero Technology Symposium*, Rep. of Korea, 31st October 2013.

[2] J.D. de Boer. Towards application of Fiber Bragg Gratings for load monitoring purposes at aircraft component level, *NLR Memorandum*, AVGS-2012-030, November 2012.

[3] J.J. Rabelo Faria. The application of Fibre Bragg Grating sensors for load monitoring of aircraft components, *NLR Memorandum*, AVGS-2013-019, August 2013.

[4] D.A. Harold, J.C. Duke, L.N. Harold. The effects of adhesive geometry and type on strain transfer for optical fiber strain sensing, *Materials Evaluation,* 1411-1419, December 2012.

[5] J.S. Hwang. Evaluation of Fiber Bragg Grating Sensors for Load Monitoring of Aircraft Components, 2014, *NLR Report*, CR-2014-121, March 2014 (under review).

[6] R.D. Finlayson, M. Friesel, M. Carlos, P. Cole, P., J.C. Lenain. Health monitoring of aerospace structures with acoustic emission and acousto-ultrasonics, *Insight*, Vol. 43, No. 3, March 2001, pp. 155-158.

[7] M. Rabiei, M. Modarres. Quantitative methods for structural health management using in situ acoustic emission monitoring, *Int. Journal of Fatigue*, Vol. 49, 2013, pp. 81-89.